Received August 7, 2014, accepted August 13, 2014, date of publication October 17, 2014, date of current version January 13, 2015.

Digital Object Identifier 10.1109/ACCESS.2014.2363949

Multisource X-Ray and CT: Lessons Learned and Future Outlook

VASILE BOGDAN NECULAES[1], PETER M. EDIC[1], MARK FRONTERA[1], ANTONIO CAIAFA[1], GE WANG[2], AND BRUNO DE MAN[1]

[1]GE Global Research, Niskayuna, NY 12309, USA
[2]Rensselaer Polytechnic Institute, Troy, NY 12180, USA

Corresponding author: B. De Man (deman@ge.com)

This work was partly supported by the National Institutes of Health-National Institute of Biomedical Imaging and Bioengineering under Grant R01 EB006837 and R01 Grant EB011785.

ABSTRACT Distributed X-ray sources open the way to innovative system concepts in X-ray and computed tomography. They offer promising opportunities in terms of system performance, but they pose unique challenges in terms of source and system technologies. Several academic and industrial teams have proposed a variety of concepts and developed some unique prototypes. We present a broad review of multisource systems. We also discuss X-ray source components and challenges. We close with our perspective on the future prospects of multisource imaging.

INDEX TERMS Computed tomography, x-rays, carbon nanotubes.

I. MULTI-SOURCE SYSTEMS

A. MULTI-SOURCE CT SYSTEMS

The term ''x-ray tube'' originates from the early days of x-ray generation and typically refers to a sub-system consisting of a single vacuum chamber with a single ''focal spot'', which is the small area on the metallic target where x-rays are produced by an incident electron beam. More generally, an ''x-ray source'' is a device that generates x-rays. We use the term ''distributed x-ray source'' for a single assembly (typically a single vacuum chamber) containing multiple x-ray focal spots or multiple x-ray sources and the term ''multi-source CT system'' for a CT system containing multiple x-ray tubes or a distributed x-ray source.

Today, most commercial CT systems are third-generation systems, consisting of a single point source and a single arc-shaped detector. CT system architectures may use multiple x-ray sources for one or more reasons: to reduce or eliminate mechanical motion; to increase the overall system x-ray power, relative to a single x-ray source in a comparable configuration; to provide complementary information (different projection lines, different x-ray energies or combinations with different detector types); to optimize the overall system x-ray usage (decreasing patient exposure); or to reduce cost of other CT scanner components. Challenges associated with multi-source CT systems include system cost and complexity, distributed source complexity, x-ray flux limitations, increased detector requirements, scatter considerations, and calibration complexity.

In the next paragraphs, we attempt to give a relatively complete, high-level overview of multi-source CT systems disclosed in literature. We follow a logic classification based on source and system topology. As such, the order in which we present the systems is not necessarily chronologic. For each system, we provide the rationale for using multiple x-ray sources and highlight its main challenges.

1) X-RAY SOURCES DISTRIBUTED AZIMUTHALLY

The best known multi-source CT systems are based on multiple beam lines, each beamline being the combination of a detector and an x-ray tube. The first concepts originate from the 1980s [1] (Figure 1). The dynamic spatial reconstructor (DSR) [2] (Figure 2) was the first real multi-beamline CT scanner, built with 14 x-ray tubes and 14 detector arrays (phosphor with image intensifier) - all activated within a 16ms period - and combined with mechanical rotation, resulting in a 4-dimensional CT dataset. More recently, a commercial dual-source CT system was introduced [3] (Figure 3).

The main rationale in all the above concepts is to improve the temporal resolution of the measured projection data to decrease cardiac motion blur: a single beamline requires a gantry rotation of 180 degrees plus the fan angle of the x-ray beam to acquire sufficient data for reconstruction; multiple beamlines reduce the required rotation interval by a factor up to the number of beamlines (depending on the azimuthal spacing between the beamlines). For example, a system with 0.35s rotation time and 50 degrees fan angle has a temporal

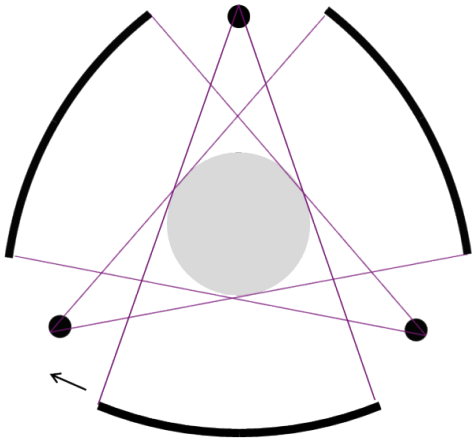

FIGURE 1. Multi-source CT system concept based on three beamlines; each beamline comprises a detector and a x-ray tube.

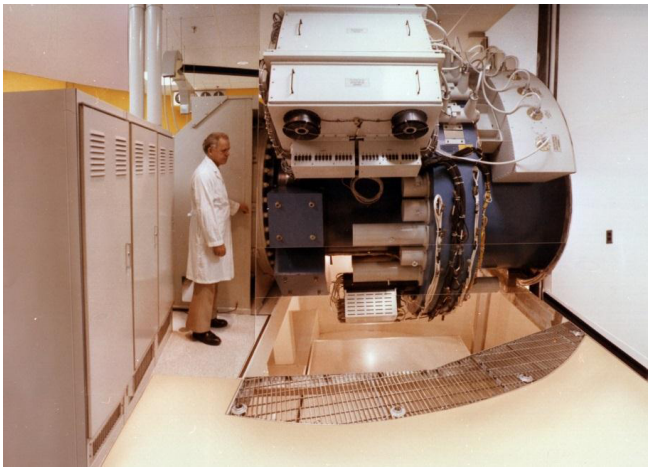

FIGURE 2. The dynamic spatial reconstructor [2] combines 14 x-ray tubes and 14 detectors, dynamically imaging a volume consisting of 240 0.75mm slices (used with permission of Mayo Foundation for Medical Education and Research. All rights reserved).

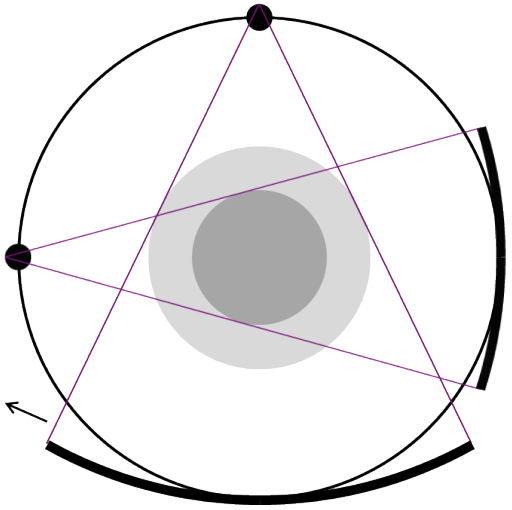

FIGURE 3. Commercially-available dual-source CT scanner consisting of two beamlines: one beamline covering a 50-cm field-of-view (FOV) and one covering part of that FOV [3].

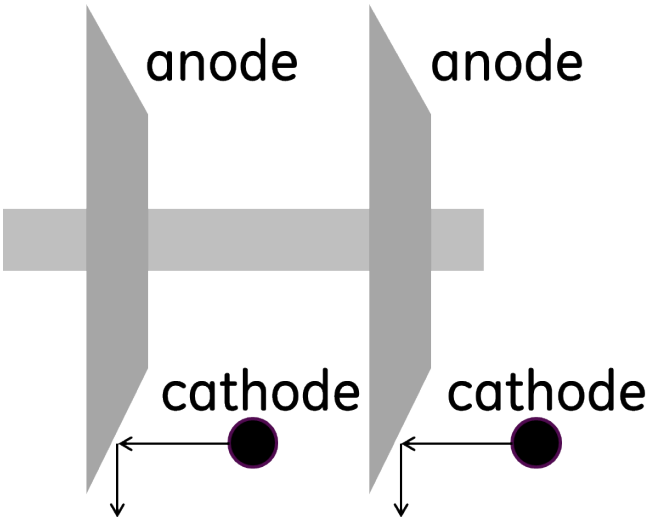

FIGURE 4. Distributed x-ray source consisting of two rotating anodes, stacked longitudinally: the respective cathodes are typically sequentially activated.

resolution of 224ms for one beamline and 136ms for two beamlines that are separated by 90 degrees. Multiple beamlines may also be used in a spiral scanning mode to reduce the total scan time of a long object [4]. Alternatively, multiple beamlines may be operated at different tube voltages, giving multi-energy imaging capability [5]. Multiple beamlines may also include different type of detectors, resulting in hybrid systems that combine standard detectors and special-purpose detectors (for example, photon-counting detectors for measurement of multi-energy projection data or flat-panel detectors for measurement of high-resolution projection data).

Since a multi-beamline CT system concept replicates several important components of a conventional scanner, the cost increases linearly with the number of beamlines. A second challenge is the limited space in a CT gantry, typically requiring limiting the field of view (FOV) of the second beamline to a fraction of the full FOV [3] and restricting the benefits of the second beamline to the corresponding smaller FOV. In interior tomography the field-of-view is restricted to a central portion of the object [94]. This relaxes the detector size requirements and makes multiple beamlines more feasible. Examples of 7, 11 and 13 beamlines with interior tomography are described in [94]. Finally, a multi-beamline CT concept causes additional scatter in projection data measurements if both beamlines are operated simultaneously, requiring an aggressive anti-scatter collimator to avoid excessive bias and noise contamination due to cross-scatter [6], [7]. Application of advanced scatter estimation/correction algorithms may mitigate this impact, but signal-to-noise ratio in the measured projection data is reduced due to the noise introduced by the scatter signal.

2) X-RAY SOURCES DISTRIBUTED LONGITUDINALLY

Several groups have proposed using longitudinally offset x-ray sources [8]–[13]. This can be achieved for example by using multiple longitudinally offset cathode-anode sets. Figure 4 schematically represents two rotating anodes

mounted on a drive shaft and two cathodes, with arrows indicating the electron beams and the x-ray beams respectively.

In some concepts, the x-ray sources share the same detector area and need to be switched alternatingly (on a view-to-view basis). In other scenarios, the detector has sufficient longitudinal extent so different sources irradiate different partitions on the detector and therefore can be active simultaneously [14], [15]. Theoretically, the case where multiple sources simultaneously irradiate the same detector area is still reconstructable, although the corresponding inverse problem is much more ill-posed. Multiplexing schemes have also been proposed to better decode this type of data [16]; however, it has been shown that this approach leads to increased noise in quantum-limited acquisition regimes [17].

A first rationale for using longitudinally offset x-ray sources is the complementary nature of the respective projection data measurements from a Radon frequencies perspective, which can be exploited to reduce cone-beam artifacts [18], [19]. A scanner may be designed for a certain longitudinal coverage (z-coverage), which is the extent of the subject that is covered in one (partial or full) rotation. The z-axis is assumed to be the rotation axis of the scanner and the x- and y-axes are the horizontal and vertical axes parallel with the central scanning plane. Since the z-coverage depends on the transaxial (xy) position, it is typically quoted at iso-center (at the rotation axis). Due to the scanner magnification, which typically is between 1.5 and 2, the detector physical z-dimension is larger than the z-coverage at iso-center, by that magnification factor. With multiple offset sources, the detector z-dimension can be reduced and still achieve the same z-coverage. This detector cost reduction is a tradeoff with the source cost increase, requiring careful consideration. In the limit, table translation necessary to cover a large volume on the patient can be completely eliminated [20].

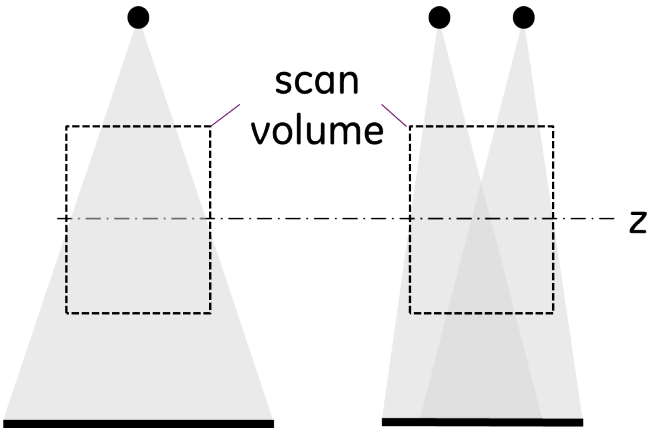

FIGURE 5. Scan volume and x-ray flux pattern for single source and two longitudinally offset sources. The latter has a reduced physical detector z-dimension for the same scan z-coverage.

The x-ray flux distribution throughout the imaging volume also needs to be considered. Figure 5 shows a comparison between a single source and a dual-source configuration in terms of coverage, detector size, and x-ray flux distribution. When the dual sources are operating in an alternating fashion with a duty cycle of 50%, the maximum average power delivery for each tube is only 50% of its capability. In regions illuminated by both tubes, this is not an issue, but other regions may have unacceptable signal-to-noise ratio due to the reduced average x-ray flux illumination. On the other hand, tube power roughly scales with the focal spot's thermal length on the anode. The focal spot thermal width and thermal length are defined by the footprint of the electron beam on the x-ray target. The focal spot optical length and optical width are the apparent width and length when viewed from the x-ray detector. This compression is referred to as line focus. Since this multi-source configuration requires narrower cone-angles, the thermal length of the focal spot on the anode can be slightly larger for a given optical length; hence, the maximum tube power is slightly higher, partly making up for the previous loss. More details on thermal aspects of the x-ray tube target are given in Section II.C. Finally, when the same detector area is irradiated by longitudinally offset sources, scatter septa between detector rows become impractical and the system is limited to a 1D anti-scatter grid, which leads to higher scatter contamination.

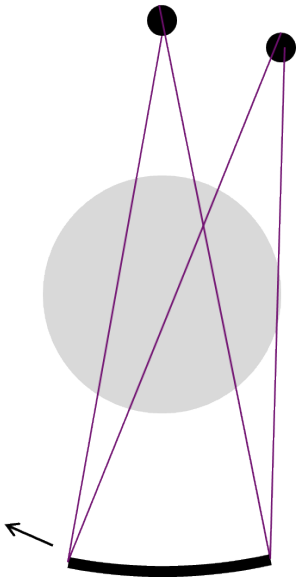

FIGURE 6. Dual-source CT concept with two x-ray tubes and one reduced-size detector, still providing full-FOV projection data after a full rotation.

3) X-RAY SOURCES DISTRIBUTED RADIALLY

Analogously, x-ray sources can be offset laterally, such that they cover a different portion of the FOV, unlike in the case of azimuthally distributed sources and detectors. This allows a proportional reduction in the detector xy-dimension (Figure 6), which may be a cost advantage. This concept can be generalized to an inverse-geometry CT architecture (Figure 7) [21]–[27], consisting of many sources and a dramatic reduction in detector size. An appealing aspect

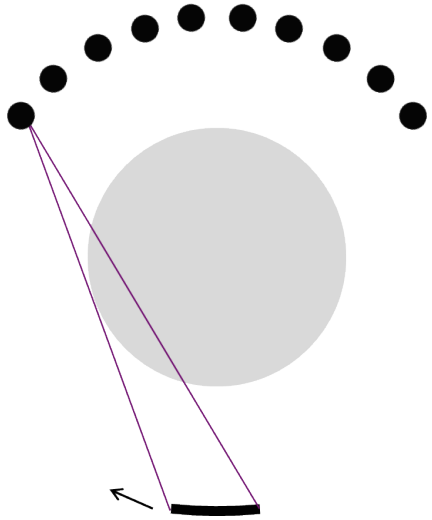

FIGURE 7. An inverse-geometry CT architecture combines a wide array of focal spots with a reduced-size, high frame-rate detector.

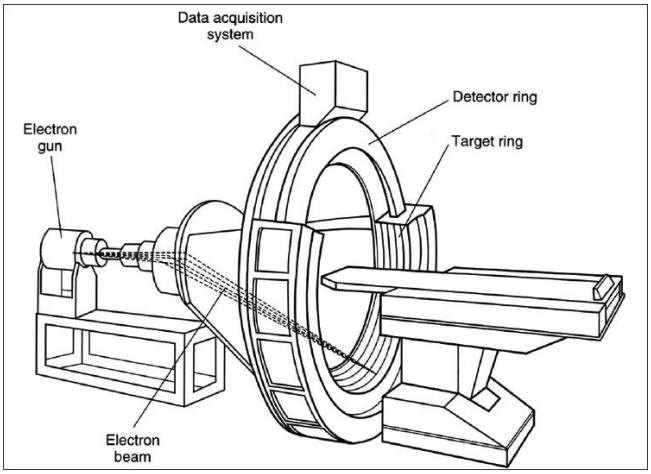

FIGURE 8. The electron-beam CT scanner has no mechanical motion: an electron beam sweeps over one of four target rings and x-rays are detected on the diametrically opposed two-row detector (Used with permission from GE Healthcare. All rights reserved).

is the complete flexibility in shaping the x-ray flux profile across the illumination field of view (virtual bowtie) by designing pulse sequences with variable tube current and voltage [24], [28]. This scheme can be extended to considering collimation schemes that illuminate only a region of interest and avoid dose-sensitive organs. A virtual bowtie can also help reduce the dynamic range of the x-ray flux incident on the detector by appropriately modulating the x-ray flux across the imaging field of view, reducing the detector dynamic range requirements, which is favorable especially for photon-counting detectors that have count rate limitations.

Similar to the source topology discussed in the previous section, the average x-ray flux through each given voxel decreases based on the duty cycle of how often the voxel is illuminated by x-ray flux. Moreover, distributed sources with a limited number of focal spots have a smaller total thermal area (the product of the focal spot thermal area and the number of focal spots) than configurations using rotating-anode x-ray tubes, and hence have lower power capability, which further exacerbates the flux challenge (see Section II.C x-ray target).

4) STATIONARY CT

A stationary CT design is defined as a system with enough x-ray sources to completely eliminate mechanical rotation. The best known example is the electron-beam CT scanner, commercialized by Imatron, which was the name of the company before it was acquired by General Electric (Figure 8) [29]. An electron beam is swept across one of 4 circular tungsten targets inside a large vacuum chamber, creating essentially a continuum of x-ray sources along an arc. This is coupled with two detector rings, diametrically opposed from the source targets.

The main motivation behind electron-beam CT was cardiac imaging with unprecedented temporal resolution. Images are reconstructed from each 50ms sweep of the electron-beam. The biggest challenge is the difficulty to expand this design to more slices and make it volumetric (large coverage on the patient, typically assumed to be at least 40 mm of longitudinal coverage), because of the inability to effectively collimate each of the x-ray source locations to the detector, as well as because of the reconstruction challenge associated with the offset cone-angle, since the geometry prohibits the x-ray source and detector from sharing the same z-position.

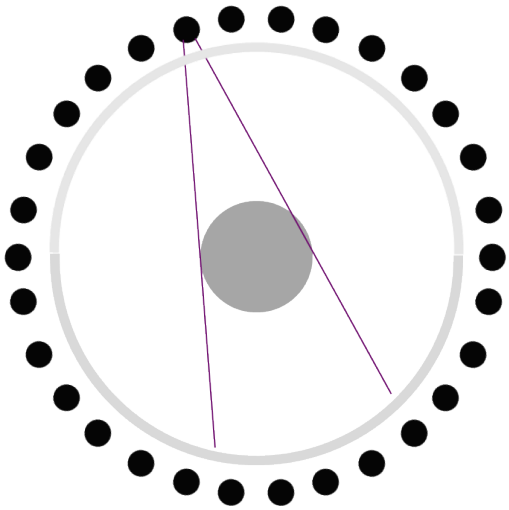

FIGURE 9. An example of a stationary CT architecture based on a full ring source and a full (longitudinally offset) ring detector.

Many stationary CT configurations were proposed based on distributed sources (Figure 9) [30]. Each x-ray source is activated to generate one view. The entire scan is performed by electronically triggering all x-ray sources, which can be performed very rapidly. In addition to improved temporal resolution, the absence of any moving parts in stationary

CT may offer improved reliability. This assumes the reliability or redundancy of each x-ray source has a longer mean time between failures than today's CT system. Furthermore, stationary CT geometry and operation enable special source trajectories, such as bit-reverse patterns [31], [32] that would be difficult to obtain by mechanical motion. A stationary CT design was implemented for luggage scanning applications [33].

A major challenge with fully stationary CT scanners is the size and cost of the source (large vacuum chamber) and detector (large number of channels). Additionally, since there is always a finite offset between source and detector, it is difficult, if not impossible, to design a stationary CT architecture that can acquire a volume with complete Radon sampling.

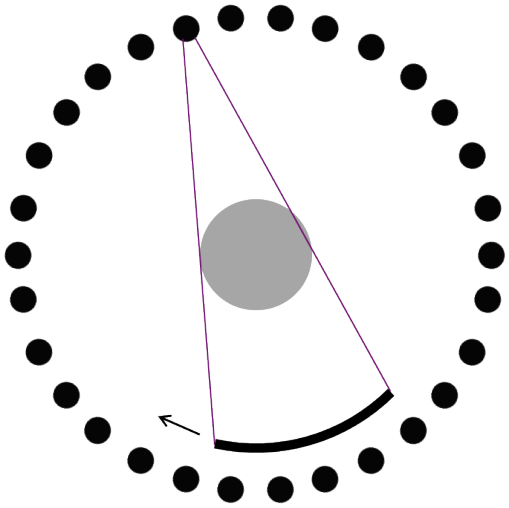

FIGURE 10. Semi-stationary CT concept with a rotating detector inside a stationary source ring.

5) HYBRID CONCEPTS

A possible compromise between a single-source CT system concept and a fully-stationary CT system is a combined rotating detector with a stationary source ring (Figure 10) [30], [34]. This topology dramatically reduces detector cost relative to a fully-stationary design. It also eliminates the Radon completeness problem, since the detector can be located inside the source ring. This can be extended to multiple detectors (for improved temporal resolution), to multiple source rings (for reduced cone-beam artifacts), and to inverse-geometry configurations [35] (for dose reduction with virtual bowtie). Furthermore, each detector can employ a collimator to reduce object scatter, thereby improving imaging performance.

Finally, some concepts have been proposed where the source and detector rotate at different rates, and even in opposite directions [36], [37]. This leads to interesting patterns in filling of the Radon space, but it is not clear whether the potential benefits outweigh the practical mechanical challenges.

B. MULTI-SOURCE X-RAY SYSTEMS

In Section I.A we considered the use of multiple sources for fully tomographic imaging using principles of CT. Here, we present published uses of distributed source technology for x-ray radiographic imaging (or ''x-ray imaging'' in short), namely for x-ray stereographic imaging and x-ray tomosynthesis imaging. For stereographic imaging, two distinct imaging beamlines, each comprising a separate x-ray source and detector, are situated on one or more gantries; these imaging system are operated simultaneously. Using well-known triangulation methods, high-contrast features in radiographic images from both imaging chains are used to derive depth information for such features in the patient or object being scanned. Additionally, these systems can be used to acquire projection data suitable for CT image reconstruction, by rotating the one or more gantries for an angular coverage of 180 degrees plus the fan angle of the x-ray beam (assuming both imaging systems are identical) – commonly denoted as a ''spin'' acquisition. When performing tomosysnthesis, or laminography in non-destructive testing applications, projection data are acquired for a limited range of angular positions of the x-ray source and detector pair about the patient or object being scanned.

FIGURE 11. Bi-plane X-ray system. Two beamlines enable stereographic imaging and faster "spin"acquisitions (Used with permission from GE Healthcare. All rights reserved).

1) DUAL X-RAY SOURCES: BI-PLANE X-RAY SYSTEMS

The conceptually, but not necessarily physically, simplest implementation of a multi-source x-ray configuration is to utilize two separate beamlines each comprising an x-ray source and detector to simultaneously acquire x-ray projection data (see Figure 11). As mentioned above, these systems are used for stereographic imaging. These systems can be rotated over a limited angular range to provide three-dimensional depth information of structures being imaged, or configured to perform a ''spin'' acquisition of projection data suitable for CT reconstruction. For ''spin'' acquisitions, the imaging chains are typically rotated much slower than standard CT imaging systems, requiring 5–10 seconds to acquire the required projection data, and utilize flat-panel x-ray detectors providing radiographic data within a limited field of view within the patient or object. The system

benefit of reduced scan time and challenge of system cost are comparable to those mentioned in Section I.A (Multi-source CT Systems: *X-ray sources distributed azimuthally).*

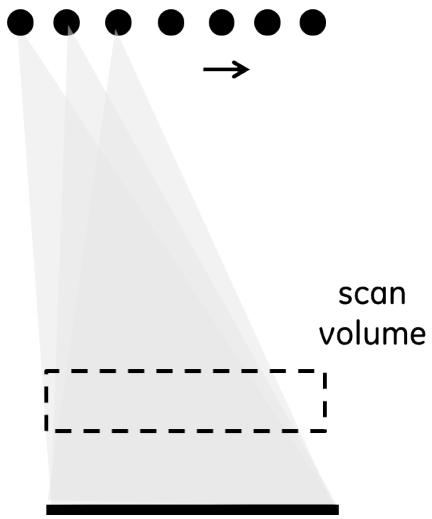

FIGURE 12. Linear X-ray source system configuration. A linear distributed x-ray source allows acquisition of tomosynthesis views without gantry movement.

2) X-RAY SYSTEMS WITH LINEAR DISTRIBUTED X-RAY SOURCES

Due to physical space limitations as discussed in Section I.A, it is not feasible to combine more than a few discrete x-ray sources to fabricate a multi-source imaging system. To realize compact distributed x-ray source systems, multiple source x-ray focal spots, typically generated by separate electron emitters, are incorporated into a single vacuum enclosure; the first systems utilized a linear configuration of x-ray focal spots (see Figure 12). These systems allowed acquisition of projection data suitable for tomosysthesis imaging without physically moving a gantry and utilized a single x-ray detector. The main technical advantages of compact distributed source systems are (1) to acquire projection data more rapidly since the gantry is held stationary during data acquisition, (2) to reduce/eliminate imaging resolution degradation due to gantry motion during data acquisition and/or patient motion during data acquisition (due to faster scan times), and (3) to simplify the system design by eliminating provisions for mechanical gantry motion [38]. Select clinical application needs may be able to leverage the benefits of distributed x-ray topologies; however, technical challenges still exist (see below), which limit wide-spread utilization.

In tomosynthesis systems for x-ray imaging, typically high-resolution, flat-panel detectors are utilized; these detectors provide high-resolution imaging in a plane whose direction is orthogonal to the x-ray beam, with the presence of intensity-diminished, out-of-plane structures. However, in the direction parallel to the x-ray beam, imaging resolution is reduced due to the limited angular coverage of measured projection data. As mentioned when discussing distributed source concepts for CT imaging, projection data from an angular coverage of at least 180 degrees plus the fan angle of the x-ray beam are required for theoretically exact CT reconstruction.

As reported in the literature for sources utilizing multiple emitters/electron beams, linear distributed x-ray source configurations used for tomosynthesis applications typically comprise tens of x-ray focal spots spread over a limited angular range (see references related to specific applications below). As such, the projection data set is mathematically incomplete for exact CT reconstruction, resulting in anisotropic imaging resolution. However, these systems provide useful imaging information when appropriately matched to the clinical imaging need. In the following paragraphs, we describe some of the reported clinical x-ray applications that have been proposed for linear distributed x-ray source technology. We detail the advantages of the technology for the given application, but, where appropriate, identify remaining technical challenges that may limit full utility of such an imaging approach.

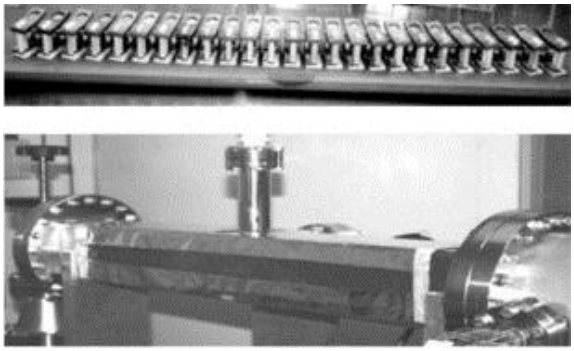

FIGURE 13. Linear distributed x-ray source for digital breast tomosynthesis. The source comprises 25 distinct focal spots (reproduced with permission from [58]).

3) DIGITAL BREAST TOMOSYNTHESIS (DBT)

DBT using a linear distributed x-ray source array is a commonly researched application of distributed source technology (see Figure 13). For DBT, the key clinical motivation for using stationary, distributed x-ray source locations is to allow fast data acquisition, resulting in reduced breast compression time and discomfort to the patient, and to improve image quality by eliminating gantry movement during data acquisition [40]. Alternatively, the resolution benefit provided by the distributed source system can be achieved with a single-source system that steps the gantry and allows sufficient motion settling time before data acquisition, albeit at the cost of overall scan duration and the mechanical complexity of the gantry. DBT is an application well-suited for distributed x-ray source technology due to the reduced power requirements of the x-ray tube (in terms of both operating voltage and beam current), a typical limitation of distributed source topologies due to the utilization of a stationary anode x-ray source configuration (see subsection *Additional Advantages and Challenges of Distributed x-ray Source Technology for x-ray Imaging*).

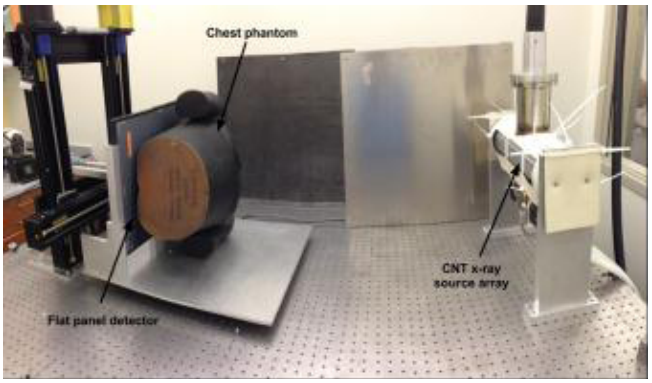

FIGURE 14. Benchtop setup modeling a digital chest tomosynthesis system (reproduced with permission from [40]).

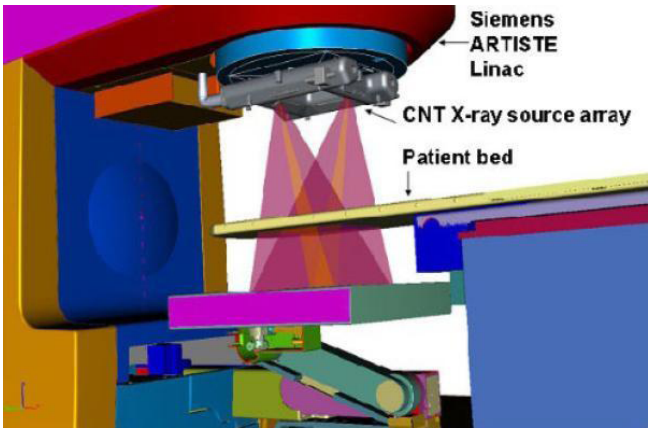

FIGURE 15. Conceptual drawing of a rectangular distributed source mounted on a radiation therapy device (reproduced with permission from [38]).

4) DIGITAL CHEST TOMOSYNTHESIS (DCT)

DCT has been proposed as another application of distributed x-ray source technology (see Figure 14). Tomosynthesis is best utilized for imaging applications requiring detection of high-resolution, high-contrast features. For chest imaging, one preferred use is in detection of lung nodules [41], [42]. The distributed source configuration allows faster scan times by eliminating gantry motion and improves imaging resolution by reducing both voluntary and involuntary patient motion (due to the beating heart or residual respiratory motion) – all subject to limitations in detector readout speed (see subsection *Additional Advantages and Challenges of Distributed Source Technology for x-ray Imaging*). The proposed advantage of tomosynthesis imaging for lung nodule detection is reduced radiation dose relative to CT image. However, before becoming a clinically-recommended procedure, a detailed clinical trial is required that shows comparable or better results in improved lesion detection and associated patient outcomes as was demonstrated in the National Lung Screening Trial – a 20% reduction in mortality from lung cancer [43], which resulted in a recommendation for lung cancer screening of high-risk patients by the U.S. Preventive Services Task Force [44].

5) IMAGE-GUIDED RADIATION THERAPY (IGRT)

IGRT is another proposed application of distributed x-ray source technology. In one configuration, four linear sections of distributed x-ray sources surround a high-energy treatment beam [38]. The distributed sources are useful for acquiring projection data and generating tomosynthesis reconstructions intermittently with therapy treatment. The resulting images facilitate tumor localization to ensure that the treatment planning regimen applies the high-energy beam as desired – to tumorous tissue, while minimizing impact on surrounding healthy tissue. One concern with using tomosynthesis imaging principles for this type of application is the low-contrast of the tumorous tissue relative to normal tissue. To facilitate the process, metal beads are inserted at locations within the tumor to facilitate organ localization [45]. The use of fiducial implants and tomosynthesis imaging are well-suited for the IGRT application – imaging of high-resolution, high-contrast structures (fiducial markers) with non-diagnostic, but sufficient, image quality suitable to meet the imaging goal - localization and tracking of the tumor during radiation treatment.

6) X-RAY SYSTEMS WITH AREA X-RAY SOURCES

A novel system utilizing a two-dimensional or area configuration of distributed x-ray source locations is an inverse-geometry x-ray imaging system [39]. The distributed x-ray source topology is a bit different from the principles that have been discussed with regard to linear distributed source configurations, which generally utilize individual, discrete electron emitters. The inverse-geometry system utilizes an x-ray source where an electron beam is continuously swept across a 23 cm × 23 cm transmission target, comprising 10,000 focal spot locations (see Figure 16). In an inverse-geometry system, the roles of the x-ray detector and the x-ray source are essentially switched – the source typically has a relatively large extent, while the detector size is dramatically reduced. The topology, when used with a photon-counting detector, increases the detective quantum efficiency (DQE) of the system since a non-segmented, monolithic crystal directly converts x-rays to electrons for subsequent collection/sampling. The system DQE is further enhanced because a detector collimator to reduce scatter is not needed since only a small percentage of the imaging volume is illuminated by a given x-ray source location at a time, and the distance between the patient and the detector is large. The system concept has already been investigated for interventional cardiology; the topology reduces skin dose to the patient by increasing the x-ray entrance angle on the patient and allows dose modulation across the imaging field of view based on patient anatomy and the imaging goal. The instantaneous power capability of the x-ray source is 24 kW, which is less than the approximately 100 kW power capability of single-source, rotating-anode x-ray source technology utilized in interventional systems with wide-spread clinical utilization.

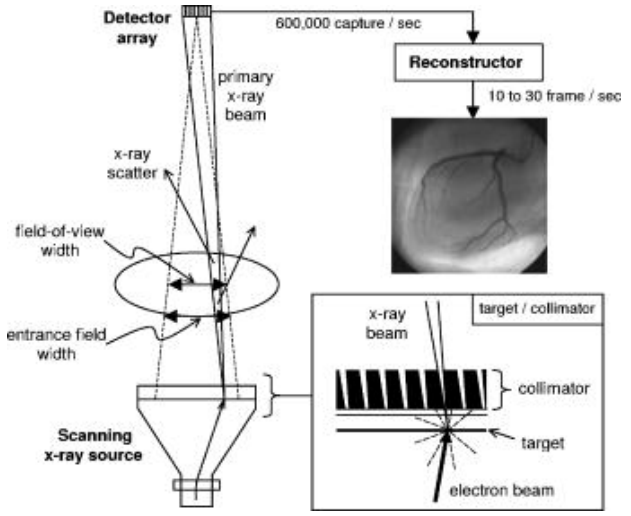

FIGURE 16. Scanning beam digital x-ray technology. A swept electron beam activates 1 of an array of 100 × 100 focal spot positions. A small percentage of the imaging field of view is illuminated during activation of each source position using a source collimator. A reconstructor combines the acquisitions to generate a radiographic view of the imaged volume (reproduced with permission from [79]).

7) ADDITIONAL ADVANTAGES AND CHALLENGES OF DISTRIBUTED X-RAY SOURCE TECHNOLOGY FOR X-RAY IMAGING

In addition to the salient benefits mentioned above, another significant benefit of distributed x-ray source technology for tomosynthesis applications is the ability to fabricate the source array in arbitrary two-dimensional configurations (three-dimensional configurations are possible within the constraints imposed by supporting anode/cathode structures to allow illumination of the imaging volume). For example, linear, square, rectangular, and circular configurations have been proposed [42]. The more complicated distributed source topologies aim at improving the sampling of projection data to further improve both in-plane and depth imaging resolution, within the constraints of the limited-angle acquisition of projection data. Especially when considering two-dimensional distributed source configurations, these topologies have a significant advantage over mechanical systems since the need for complicated two-dimensional motion controllers is obviated.

Some challenges still remain for tomosynthesis imaging utilizing distributed x-ray source technology. As mentioned above, typically high-resolution, flat-panel detectors are utilized in such systems. The pitch of individual detector cells of flat-panel detectors is typically 100um to 200um in each spatial direction. Since millions of pixels comprise the detector subsystem, sequential digitization of stored charge within a subset of detector cells comprising either rows or columns of the detector is performed to reduce the complexity and cost of associated digitizing electronics. Although a cost-effective solution, a drawback of this subsystem architecture is that the fast data acquisition provided by a distributed x-ray source is not fully realized due to detector digitization/readout time.

An additional challenge of distributed source technology is output power capability of such x-ray source architectures. When considering individual components of the distributed x-ray source and the x-ray target in particular, as discussed in Section II.C, the use of both reflection and transmission topologies for electron beam bombardment on the anode typically favor a configuration where the anode is held stationary. As such, the quiescent power of the x-ray tube is reduced unless hundreds of distributed focal spots at very short dwell times are employed. Such a scheme places further demands on detector readout speed.

II. DISTRIBUTED SOURCE TECHNOLOGIES

A. ELECTRON EMITTERS AND ELECTRON BEAM OPTICS

This subsection will mostly focus on electron emitters and beam optics for distributed sources with multiple electron beams. From the emitter point of view (packaging and beam optics) these sources tend to have a much higher degree of complexity, along with specific challenges, compared to traditional scanning electron beam sources – that rely on one cathode/electron emitter, one electron beam that is deflected to predetermined spatial locations on the x-ray target [29], [39].

Commercial x-ray tubes tend to employ tungsten-based electron emitters, in coil (most cases) or flat emitter [46] architectures. These tungsten emitters are typical heated towards 2500 °C for thermionic emission using tens of watts of heating power. Commercial medical x-ray sources function in the temperature limited regime – to adjust emission properties, one needs to change the temperature of the emitter (this process has a time constant on the order of millisecond). Since most diagnostic imaging x-ray sources are sealed, the pressure during operation reaches 10^{-5} Torr, which is acceptable for tungsten emitters. Beam optics design in most commercial x-ray sources tends to be fairly simple, based on focusing tabs (line emitter, line thermal focal spot on the target) at potential which help to shape the electron beam profile.

Commercial x-ray tubes may have one or two electron emitters or cathodes with only one emitter activated at a time. Two separate electron emitters (only one is turned on at a time) may be employed to generate a small and a large focal spot, or to generate x-rays using two different target tracks – molybdenum and rhodium or bi-angle, for example. A distributed x-ray source may employ a much larger number of emitters, from tens to even hundreds of cathodes. As such, a compact distributed source with a very large number of tungsten emitters all heated at more than 2500 °C and dissipating tens of watts of heating power is not feasible. The ideal electron emitter for such distributed sources is the field emitter: a cathode that generates electrons at room temperature, upon application of a large electric field proximate to its surface. A large number of cathodes in a single, compact vacuum chamber, generating electrons at room temperature will not pose any thermal management challenges for the electron guns comprising an emitter and electron beam focusing hardware. Therefore, field emission technology is a key enabler for a distributed source with a

large number of cathodes and will be subsequently discussed in more detail.

Typical field emitter cathodes rely on high aspect ratio physical shapes – Carbon Nano Tubes (CNTs), or metallic micro-cones (Spindt type emitters) – for field enhancement; the field enhancement factor indicates the electric field increase at the tip of the emitter compared to a flat emitting surface; this increased electric field is the enabler for field emission. As an example, the high aspect ratio of CNTs is obvious when we take into account their length on the micron or higher range while their diameter is a few nanometers to tens of nanometers [47]. Traditional Spindt emitters comprise metallic molybdenum cones with a height about 1-2 microns and a tip radius of tens of nanometers [48].

The scientific community has investigated a very large number of materials as field emitters – well beyond CNTs or Spindt micro-cone emitters made from molybdenum. Several examples are: ferroelectric ceramics [48], carbon fibers as explosive electron emission sources [48], silicon nano structures [49], zinc oxide nanowires [50], silicon carbide nanorods [51], silicon carbide nitride nanorods [52], graphene [53], graphene oxide sheets [54], etc. This paper is not a field emission review; however, this sampling of materials investigated for field emission shows that this research area is continuously searching for the ideal field emitter: a material with low turn-on field (the electric field that needs to be applied to trigger the electron emission), with excellent current density (at least 1 A/cm^2 or higher) and long lifetime (robustness to vacuum contaminants and the high voltage discharges that are typically encountered in x-ray sources). While many of these field emitter materials have been already used in proof of concept x-ray emission experiments, distributed x-ray source prototypes utilizing cold cathodes (cathodes that utilize principles of field emission) have focused mainly on utilizing Spindt and CNT emitters.

1) SPINDT EMITTERS

With more than 40 years of research, Spindt emitters are some of the most well-known and characterized cold cathodes. These emitters have demonstrated current densities up to 40 A/cm^2 and a lifetime of 10,000 hours at a current density of approximately 1 A/cm^2 (albeit at a collector voltage of 1 kV, much lower than typical high-voltage conditions in an x-ray source) [55]. Recently published results for a linear distributed source with 10 cathodes with 1 cm spacing, focus on demonstrating imaging performance using a mouse phantom [55]. Source characterization mostly utilized lower operating voltages up to 50 kVp. While typical cathodes showed good lifetime at 1 A/cm^2 (10 mA total current), some cathodes were tested up to 10 A/cm^2 (100 mA total current). Experimental learnings from this study indicate that Spindt technology may not be ready yet for commercial deployment. Historical data suggest lifetime limitations if current density is increased beyond 1 A/cm^2 [55]; therefore, any commercial embodiment may need to focus on clinical applications requiring this current density. The very high vacuum typically used in these experiments – five orders of magnitude higher than commercial sealed x-ray source technology operating at about 10^{-5} Torr – as well as the long processing and conditioning time required by these emitters, on the order of few days, are additional hurdles for commercialization. More research needs to be done in understanding failure mechanisms of these emitters in an x-ray tube environment; the linear distributed source study used about 200 cathodes, and about 100 cathodes suffered failures (some 50 showed catastrophic failures) [55]. Time to failure was anywhere from 10 minutes to more than 50 hours. However, some failure mitigation approaches (see Figure 17, reproduced from Physics in Medicine and Biology) [55], showed great promise. Since one of the failure mechanisms for Spindt emitters consists of gate electrode to emitter tip shorting, the implementation of a dielectric shield right beneath the gate seems to significantly reduce failure rates.

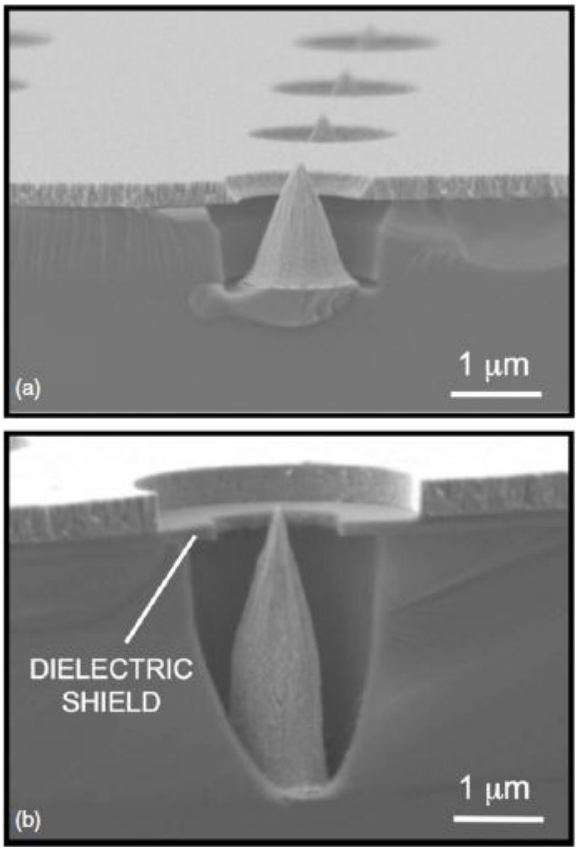

FIGURE 17. Typical spindt cathode (a) and improved Spindt design (b) with dielectric shield to prevent gate electrode to emitter tip shorts (reproduced with permission from [55]).

2) CARBON NANO TUBES

The other field emission technology extensively studied in distributed x-ray sources is based on CNTs. The research group at University of North Carolina led by Otto Zhou, in collaboration with various commercial entities or other academic institutions, has been extraordinarily prolific in the fabrication of CNT based x-ray sources for more than a

decade, from proof-of-concept experiments to exciting prototype demonstrations (one example is presented in Figure 18). Several distributed source demonstrations by this group include a multi-pixel array (5×10 array on a CNT chip) x-ray source for micro-radiation [56], breast tomosynthesis in 31-source [40], [58] and 25-source embodiments [57], [59], 52-emitter source for image guided radio therapy [38], a 75-spot linear source for tetrahedron beam computed tomography (for image guided radiotherapy) [60], and a 75-spot linear source for chest tomosynthesis [41], [42].

FIGURE 18. CNT based breast tomosynthesis system (reproduced with permission from [62]).

At the heart of these source embodiments are the CNT field emitters. While CNT basic science research has been ongoing for more than 20 years, there is no large scale, successful commercial application of this field emission technology. While various researchers have investigated failure mechanisms of CNTs [47], the level of understanding for CNT emitter reliability is less advanced compared to commercially-available thermionic cathodes. While publications detailing distributed x-ray source concepts utilizing Spindt device have been rich in providing details regarding failure mechanisms [55], failures rates, lifetime versus emission density tradeoffs, lifetime at low and high voltages on the electron collector/target, vacuum contaminant effects on lifetime, and challenges for large-scale commercialization, comparable information for CNT cathodes has not been published yet. Therefore one cannot make a direct comparison between the two cold cathode approaches in the context of distributed x-ray source applications. However, it seems that the CNTs tolerate 2-3 orders of magnitude higher pressure [59] compared to Spindt cathodes [55] – a significant advantage when considering potential commercialization.

The CNT source prototype for breast tomosynthesis [40] used 2.5 mm $\times$ 13 mm area cathodes. The length of the linear source comprising 31 separate cathodes is 370 mm. CNT cathodes demonstrate good emission reproducibility, as well as excellent lifetime when operated at 38 mA total current, although the target voltage is not specified. This corresponds to a current density of about 0.1 A/cm^2; Spindt emitters claim reliable lifetime around 1 A/cm^2 typically, including operating in an x-ray source. Future research could explore lifetime performance of CNT emitters in an x-ray source setting that operates the emitters at higher current densities. It should be mentioned that the same group recently reported a 4A/cm^2 CNT cathode with excellent lifetime [61], although not integrated in an x-ray source.

Finally, the 75-source linear prototype [60] uses 1×20 mm^2 CNT cathodes separated by 4 mm; each cathode generates 3 mA, which corresponds to a current density of about 0.01 A/cm^2.

3) DISPENSER CATHODES

While the great features of cold cathodes may change the future direction of x-ray source design, they may not be yet ready for x-ray source commercialization. An electron emission technology far more mature than field emitters and with some practical advantages compared to traditional tungsten cathodes for distributed sources is the dispenser cathode [68]. A traditional presence in vacuum-based microwave amplifiers in the last few decades, dispenser cathodes have demonstrated excellent electron emission and lifetime properties. These cathodes are a class of thermionic emitters, required to be heated to produce electrons; however, they require much lower heating compared to traditional tungsten cathodes. Dispenser cathodes need about 1000 °C to emit electrons. Therefore, distributed sources with tens of dispenser cathodes should be feasible, although a source with a larger number of cathodes (>50-100) will not be easily demonstrated with these emitters due to electron gun thermal management issues.

GE Global Research has successfully demonstrated distributed sources with dispenser cathodes for Inverse Geometry CT (IGCT) [25], [42], [63]–[68]. The source was designed for 32 (Figure 19) spots in two linear arrays [68] – each linear array comprising 16 cathodes – but was initially demonstrated experimentally on a reduced scale, with 8 spots [67]. To date, this is the only published x-ray distributed source demonstrated on a rotating gantry; additionally, the dispenser cathode based IGCT source achieved beam currents on the order of hundreds of mA from a 3.5 mm diameter cathode (more than 1A - 10 A/cm^2 - demonstrated in bench top experiments). This source was operated reliably for hundreds of hours. In terms of reliability, manufacturability, conditioning, emission current density, lifetime, robustness to high voltage activity, dispenser cathodes are a viable option to state-of-the-art cold cathode technology; however, as mentioned above, sources requiring a large number of cathodes require cold cathode devices. In terms of vacuum conditions, CNTs and dispenser cathodes seem to require relatively similar vacuum levels, significantly higher and easier to implement when compared to vacuum requirements of Spindt emitters. Finally,

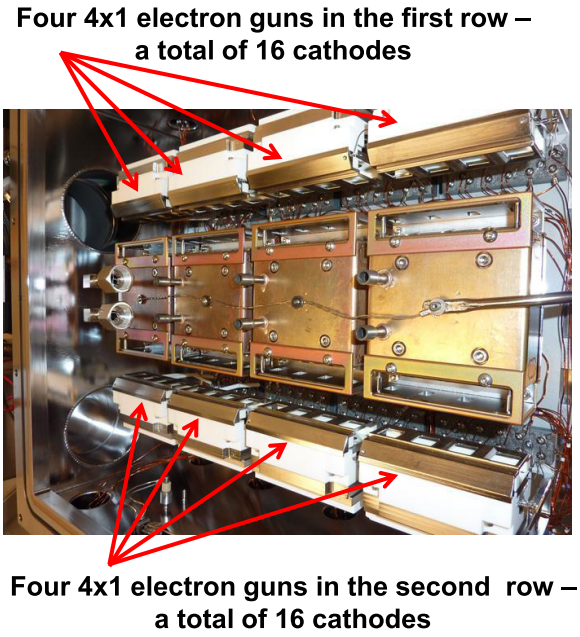

FIGURE 19. 32-spot distributed source demonstrated at GE Global Research, reproduced with permission from V. B. Neculaes, Y. Zou, P. Zavodszky, L. Inzinna, X. Zhang, K. Conway, K. Frutschy, W. Waters and B. De Man, "Design and characterization of electron beam focusing for x-ray generation in novel medical imaging architecture," Physics of Plasmas, 21, 056702, 2014 [68], Copyright 2014, AIP Publishing LLC.

it should be mentioned that the x-ray source used in electron-beam CT, a distributed source with one scanning electron beam (see section I.A), also uses a dispenser cathode.

4) ELECTRON-BEAM OPTICS

Electron-beam optics is a critical function in x-ray sources. Electron-beam focusing directly influences imaging resolution (assuming that the detector is not the limiting factor). When source embodiments include multiple cathodes, architectures for providing electron-beam optics based on magnetic focusing may not be easily feasible due to extreme space limitations [68]. The discussion here focuses mostly on electron beam optics for multi-beam distributed sources – the novel development of the last decade. Therefore electrostatic focusing schemes using typically two focusing electrodes have been selected when working with CNTs, Spindt emitters, or dispenser cathodes [55], [57], [68]. Electron guns traditionally include, besides the two electrostatic focusing electrodes, one additional electrode for beam extraction and control. While Spindt emitters have a micro-fabricated electrode - a gate electrode integrated into the cold cathode design (triode structure), for CNT [59] and dispenser cathode [68] based distributed source architectures, a mesh grid is used for beam extraction and control. The microscopic gate integrated with the field emitter structure seems like an ideal solution; however, gate-to-emitter shorting is a major failure mechanism for micro-fabricated triodes [55].

In terms of electron beam optics, a direct comparison among various electron guns is challenging, since some groups design focusing schemes for mammography applications (less than 1 mm optical focal spot, tens of mA current), while other groups considered focusing arrangements for CT applications (∼1 mm optical focal spot, hundreds of mA currents). The CT multi-source gun utilizing dispenser cathodes has shown a compression ratio of about 30 at 30 mA [68], while the CNT electron gun for breast tomosynthesis has an inferred beam compression of about 25 at 38 mA [40] – comparable performance at tens of mA. The beam compression is calculated as the area of the cathode divided by the area of the thermal focal spot, indicative as to how the initial electron beam profile is compressed by the time the electrons hit the target. It should be mentioned, however, that the electron beam optics for the breast tomosynthesis CNT-based electron gun developed in [40] delivers a focal spot of 0.6 mm, which is larger than current commercial offerings.

5) OTHER CONSIDERATIONS

Typical triode structures – micro-fabricated (Spindt) or macroscopic (CNT, dispenser cathodes) – will lose some of the emitted current at the gate electrode (instead of going to the target to create x-rays). For Spindt electron emitters, the gate current is very small, less that 1% of the emitted current shunts to the gate electrode [55]. The demonstrated distributed source utilizing dispenser cathodes shows that about 12-18% of the emitted current is collected by the grid electrode [68], while the CNT electron gun utilized in the breast tomosynthesis system has about 30% of the emitted current captured by the extraction electrode [59]. Larger current lost at the grid does not only mean less beam current available at the target for x-ray generation, but also thermo-mechanical concerns for the grid/gate (grid/gate heating, potential grid deformation with effects on beam optics, etc.).

Finally, the packaging of electron guns seems to involve modules [68] (Figure 19), or individual electron guns per emitter [62] (Figure 18). Serviceability in the field to address potential cathode failures makes the individual electron gun emitter choice [62] more practical. The module with four dispenser cathodes in a block gun [68] was designed in order to successfully tolerate temperatures of several hundreds of C, since the cathodes would be kept heated at about 1000 C during source operation. The design of a cold cathode electron gun does not need to consider these thermo-mechanical constraints; therefore, it is simpler and cheaper. However, cold cathode emitters may need protection against ion bombardment and high-voltage arcs, while dispenser cathodes are fairly robust against these concerns (this protection will need to be implemented in the electron gun).

B. HIGH-VOLTAGE CONTROLS

The control system of a distributed source has the essential function of turning the electron beam(s) on and off at the required pulse width, amplitude (current extracted from the emitter using an applied voltage), and frequency, as well as beam focusing. These parameters are influenced by target thermals, detector specifications, and imaging protocols. As mentioned previously, typical commercial x-ray

sources work in temperature limited regime – one adjusts the emitter temperature in order to change the electron beam current. To have the ability to pulse the electron beam quickly, one needs to use cathodes where the emission is controlled by an extracting electrode (micro-fabricated gate or macroscopic grid) placed proximal to the emitter. The emitted current is adjusted by the voltage applied to the extraction electrode alone; the electron emission is decoupled from the target accelerating voltage. These types of control architectures have the ability to turn on the electron beam in less than 1 microsecond. Scanning-beam distributed sources include one electron beam [69] that is moved/deflected to different locations on the target [29], [39]. The complexity of controlling a large number of different electron beams is a specific challenge addressed in the last decade by several research groups. Since this is truly the novel aspect in terms of controls for distributed sources, we will focus this section on briefly analyzing CNT and dispenser cathode based sources with multiple electron beams (published information regarding the control design for the distributed source utilizing multiple Spindt cathodes is limited).

Two main embodiments for multi-source controllers have been proposed in literature. The first embodiment has been used mostly for CNT-based distributed sources [40], [56], [57], [59], [60], [70] while the second embodiment mostly focused on demonstrations with dispenser cathodes, which needs to consider beam extraction and control, as well as cathode heating [25], [64], [67], [68], [71].

The controllers reported in [40], [56], [57], [59], [60], and [70] operate multiple CNT cathodes to create multiple electron beams. They connect each CNT emitter to the drain pin of a high-voltage MOSFET (High Voltage Metal Oxide Semiconductor Field Effect Transistor) switch through a resistor. There is only one grid/beam extraction electrode that is shared by all CNT emitters. Resistors in series with the MOSFET drain pin and the cold cathodes are added to compensate for the variance in performance of the different CNTs by limiting the emitted current through a negative feedback mechanism. The maximum current measured using this controller is 18 mA [59], and 38 mA (183 ms pulse duration) in a different set of experiments [40].

The controllers used in [25], [64], [67], and [68] have been demonstrated utilizing dispenser cathode based emitters (emitter heating of $\sim$10 watts per cathode, beam extraction, and control capability) and they use a different high-voltage switch approach (IGBTs - Insulated-Gate Bipolar Transistor). When eliminating the heater electronics, this controller topology can be applied to CNT/cold cathode based distributed sources as well. The maximum dispenser cathode current reported in [64] is approximately 1000 mA for a pulse width of 30 microseconds. The turn on/rise time is about 400 nanoseconds. [67] mentions an emitted current of 125 mA and pulse width of about 5 microseconds for each dispenser cathode. The matrix control of electron emitters is achieved by electrically connecting multiple emitters to the same electrical line and by using multiple grid/beam extraction electrodes [64], [71]. To be able to emit current, an emitter in a matrix configuration needs to be both "enabled" (electrically biased for emission) and its corresponding grid/beam extraction electrode needs to be at the proper potential.

Given a certain number of emitters to control, the matrix approach allows a dramatic reduction in the number of electrical lines that connect the control system to the vacuum chamber, where the electrons guns are located. For example, to control the 75 CNT-based emitters as described in [60] with a matrix approach, only 18 wires/electrical connections are required: in a matrix configuration there will be 9 rows of CNTs and 9 independent grid/extraction electrodes. To control the same numbers of CNTs using the control topology proposed in [56], [57], [59], [60], and [70] the number of electrical connections required is 76 - more than 4x, adding cost and complexity to the source. The reduction in electrical connections becomes even more dramatic when there are a large number of emitters to control, for example 100 emitters require 20 vacuum feed-through connections versus 101 without matrix control - a reduction of a factor of 5. Additionally, the matrix architecture reduces the number of high voltage switches (MOSFET or IGBT) needed.

Besides exhibiting less complexity and cost by using the matrix layout, the control topology demonstrated initially on dispenser cathodes [25], [64], [67], [68] enables higher current applications since high-voltage IGBT devices conduct more current than high-voltage MOSFET devices, utilized in the multi-source CNT control architecture [40], [56], [57], [59], [60], [70]. Finally, only the dispenser cathode control architecture can change the grid voltage from emitter to emitter and therefore the emitted current from cathode to cathode, allowing the implementation of a virtual bowtie [67].

C. X-RAY TARGET

Most x-ray sources used in medical diagnostics today are based on a rotating target/anode topology, design solution demonstrated in the Coolidge x-ray tube patented in 1917 [72]. Electrons are accelerated across a gap between the cathode and target/anode using an applied voltage from tens to more than one hundred kV. X-rays are generated when electrons are decelerated by striking a rotating surface of high atomic number material, typically tungsten supplemented with rhenium to improve reliability (this prevents cracking due to thermal cycling). The main trade-offs in x-ray tube design are the total x-ray photon output and the size of the region of x-ray generation/electron beam footprint on the anode or target (also named thermal focal spot). More photons can be created by increasing the electron beam power, but this is limited by target melting and/or rapid evaporation, and/or lifetime degradation due to thermal cycling. One could prevent target melting by increasing the thermal focal spot size; however, this may cause a larger optical focal spot with consequences in degraded image resolution.

The design of distributed source x-ray targets optimizes parameters such as system geometry, x-ray detector

acquisition speed, electron beam footprint on the target/thermal focal spot, total photon output, target evaporation, and target structural reliability. The x-ray target is one system limiter of spatial resolution, temporal resolution, and coverage. In an ideal system, the origin of the x-ray flux is treated as a point source to maximize spatial resolution. In reality, this region must have a finite area to decrease the maximum heat flux on the target/anode for x-ray generation. The temporal resolution and coverage of an imaging system may be constrained by the minimum detected x-ray signal required for each acquisition window.

Two limits of x-ray target loading are maximum operating temperature (defined as the peak temperature of the target surface) and maximum thermo-mechanical loading (defined as the maximum strain or stress in the region of x-ray generation). As the surface temperature of the target increases, the evaporation rate of the target material increases. This decreases the high voltage stability of the x-ray source and increases the probability of unintended high-voltage breakdowns via vacuum contamination. Excessive temperatures (>2600 °C) will lead to target surface melting. A localized temperature gradient creates high stresses in the target surface and assembly, leading to crack formation, crack propagation, material separation, and failure of the target assembly.

By neglecting the in-plane heat dissipation, target temperature rise may be approximated by [73]:

$$T_{Impact} = \frac{2P}{Area}\sqrt{\frac{t_{Dwell}}{\pi \rho c_p k}}, \quad \text{where } \frac{Focal\ Spot\ Radius}{2\sqrt{\frac{kt_{Dwell}}{\rho c_p}}} > 1.5$$

where P is the electron beam power deposited in the focal spot and $Area$ is the thermal focal spot area (c_p is the specific heat, k is thermal conductivity and ρ is the density of the target material; t_{Dwell} is the dwell time of the electron beam on a specific location of the target).

This is defined as the temperature rise in the focal spot, above the average target temperature, while irradiated by the electron beam. Total target temperature will be the sum of the average temperature plus the temperature rise from equation 1.

Following a single electron beam pulse, the x-ray target surface typically returns to an average temperature after approximately 2 milliseconds [74]. A more accurate temperature distribution compared to equation 1 may be predicted using finite element analysis modeling software and more precise estimates of volumetric heat deposition, temperature dependent material properties, etc.

One approach to increase the maximum electron beam power loading of distributed source x-ray targets is to decrease the dwell time and increase the number of spots (see example of calculations in Figure 20). The x-ray detector sampling frequency defines the instantaneous electron beam power loading time period/dwell time on the x-ray target. A shorter acquisition period enables a shorter duration of high-power heat generation on the target. For example, a 40 spot system, operating at a 10 microsecond x-ray generation period can sustain a beam current of 368 mA, but is limited to 136 mA if operated at a 200 microsecond x-ray generation period. If the number of spots is increased to 200, a 10 microsecond x-ray generation period can sustain a beam current of 620 mA [75]. The number of focal spots defines the target duty-cycle; more x-ray spots decrease the average power in a local section of the target.

Various distributed source concepts demonstrated experimentally use stationary targets: reflection or transmission targets. Reflection targets can include actively cooled or uncooled architectures. One design was based on a copper block with oil cooling channels; x-ray generation target plates were brazed onto the copper block [75]. Reflection targets can accommodate larger electron beam powers due to the angled structure (see Figure 2 in [68]); in these arrangements, the thermal focal spot is much larger than the optical focal spot; larger thermal spot can receive increased electron beam power for x-ray generation, but the small optical spot obtained with proper target angle ensures the needed image resolution.

Transmission targets are constructed by applying a thin layer of high atomic number material to a substrate of low atomic number material. The x-rays are generated in the high atomic number region and pass through the low atomic number region with minimal filtration and absorption. Thin transmission targets have a higher x-ray production efficiency [76]. The overall x-ray output of transmission targets is decreased compared to reflection targets, when heat flux limits are considered. Additionally, due to the fact that thermal and optical spots are identical for transmission targets, more aggressive electron beam focusing schemes are needed. Finally, transmission targets can be suited for increased source compactness; a distributed x-ray source with a large number of spots can be easier accommodated on a reduced footprint with transmission targets, as opposed to reflection targets.

In conclusion, reflection targets have the advantage of increased thermal capability and relaxed requirements for electron beam focusing compared to transmission targets. On the other side, transmission targets are more compact (decreased spot to spot spacing) and display a higher x-ray production efficiency.

1) EXPERIMENTAL & COMMERCIAL DISTRIBUTED, STATIONARY X-RAY TARGETS

Multiple groups have predicted and demonstrated engineering design limits of distributed source x-ray targets. Table 1 summarizes the application, target type, and performance of the main distributed source concepts demonstrated experimentally. Performance metrics are extracted from references [75], [77], [78], [73], [79], and [55]. The maximum electron beam loading (electron beam power on the thermal focal spot expressed in kW/mm^2) should be considered an approximation (it does not include any estimation of focal spot electron intensity distribution).

Additional teams have been exploring distributed x-ray source concepts, including Radius Health [81], Stellarray

TABLE 1. Overview of commercial and research prototypes for distributed x-ray sources.

Organization	Application	Target Style	Focal Spot [number, thermal size, dwell time]	Peak Power [kW]	Maximum Electron Beam Loading [kW/mm^2]
GE Multi-Source [75,64, 90, 66, 67]	General-purpose CT	Reflection	32, 1 mm x 10 mm	75	7.5
GE Imatron [77]	Cardiac CT	Reflection	2800, 1 mm x 12 mm, 17 us (estimated)	140	12
XinRay [78]	Mammography	Reflection	31, 0.6 mm x 2.2 mm, 250 ms	1.8	1.4
XinRay [74]	Micro CT	Reflection	10, 0.1 mm x 0.5 mm, 10 ms	0.15	3
NovaRay [79-80]	Interventional x-ray	Transmission	10,000, 0.6 mm diameter, 1 us	24	67
SRI [55]	Tomosynthesis	Reflection	10, 0.3 mm x 0.88 mm, 1 ms	1.6	6

[82], and CSEM [83]; these concepts are not discussed here. Equation 1 may be rewritten to calculate power per unit focal spot area (thermal spot). This loading intensity number is estimated as the incoming electron beam power divided by the thermal focal spot area. The maximum electron beam power density is limited here by maintaining the maximum target temperature below 2600 °C - see Figure 20. This estimation does not include design constraints from bimetallic joint thermal analysis or detailed thermo-mechanical analysis. Three scenarios (500 °C, 1000 °C, and 1500 °C) are plotted in Figure 20, representing different average target temperatures, the base temperature upon which the impact temperature rise (Equation 1) is superimposed. For reference, traditional rotating CT x-ray targets sustain a loading intensity of 10–12 kW/mm^2 and peak power of 100-120 kW. Rotating mammography x-ray targets operate at a loading intensity of 15 kW/mm^2 and peak power of 3 kW. Stationary micro-focus targets used for industrial inspection operate at a loading intensity of 5 kW/mm^2 and peak power of 150 W.

The experimental and commercially available systems shown in the table above follow the trend defined in Figure 20.

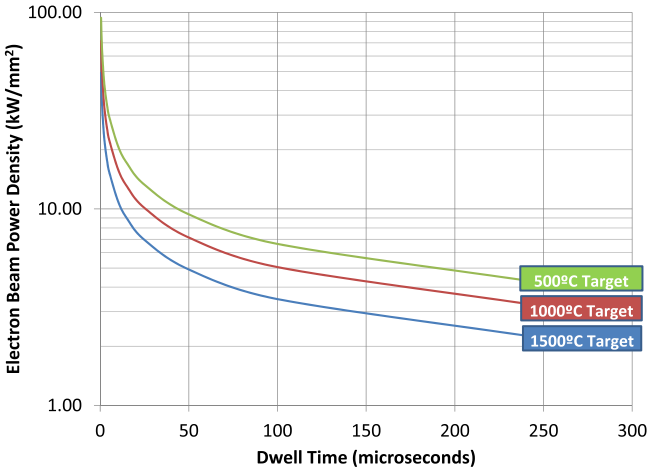

FIGURE 20. Estimation of peak power density (Equation 1) as a function of pulse width/dwell time, for 2600 °C peak temperature limit (this peak temperature is the sum between average target temperature plus the instantaneous increase in temperature due to electron beam irradiation from Equation 1). As the average target temperature decreases, one could put larger power densities on the target for the same pulse widths/dwell times and therefore increase the x-ray photon generation; however, there is also increased thermo-mechanical loading in this case, due to cyclical heating that may affect the lifetime of the target.

An increase in power density may be gained by decreasing the average temperature of the target. This will increase the mechanical loading and must be accounted for in mechanical reliability analysis.

2) FUTURE IMPROVEMENTS TO X-RAY OUTPUT CAPABILITY OF DISTRIBUTED, STATIONARY X-RAY TARGETS

Alternate approaches to increase the maximum electron beam power loading on an x-ray target have been proposed recently. Examples of these concepts include: increasing the conductivity of the target volume [84], replacing the stationary solid anode with a liquid metal jet [85], replacing the stationary solid anode with a rotating drum [86], replacing the stationary solid anode with oscillating motion [87] and enabling higher structural loads by modifying the surface of the target [88, 89]. While encouraging, these ideas require significant research and development to quantify the performance improvement, cost, and engineering risk for implementation to a distributed x-ray source. Solutions with improved heat transfer and mechanical compliance (diamond composite targets, liquid metal, variations of transmission targets, patterned target surfaces, etc.) may be challenged in maintaining x-ray output, due to the use of lower atomic number target material, increased absorption and/or filtering. Solutions with active components (rotating drum, oscillating target) may have unfavorable cost, geometry and focal spot motion.

These solutions, or another step-change in enabling higher x-ray flux density, may support simpler system level designs and expand the clinical applications and patient benefits of distributed x-ray sources.

III. FUTURE PROSPECTS

While multi-source CT designs offer a wealth of opportunities, they also have increased complexity. Other CT technologies have evolved dramatically in recent years and brought some of the opportunities within reach without using distributed sources. With gantry speeds below 0.3 s per rotation and advances in motion correction, temporal resolution has vastly improved and it is not clear how much benefit a dual-source CT architecture still offers. Sophisticated cone-beam reconstruction algorithms can effectively eliminate cone-beam artifacts up to 16 cm z-coverage, reducing the need for longitudinally offset sources. With iterative reconstruction, efficient detectors and optimized scan protocols, radiation dose is already dramatically reduced, expecting diminishing returns from the virtual bowtie concept. Fast kV switching

x-ray generators and energy-sensitive detectors offer multi-energy without going to multiple beamlines. Reduction in per-channel detector cost makes it less advantageous to use multiple sources for reduced detector size.

The promise of multi-source CT may be in high duty-cycle applications, such as luggage scanning, where reliability is an important issue. It may also have a future in ultra-fast CT applications, such as small animal imaging [93], multi-phase flow measurements [94], visualization of combustion processes, engine imaging, etc.

With the recent development of interior tomography, theoretically exact and numerically stable local CT reconstruction has been made feasible from truncated projection data that are associated with x-ray paths through a region of interest (ROI) only [91]. This approach opens possibilities for tight integration of multiple pairs of x-ray sources and detector pieces into a gantry to target a specified ROI [92]. When the performance and cost of novel x-ray sources become practically acceptable, it is imaginable to have dozens of sources fit into a gantry along with corresponding detectors for ultrafast CT imaging, especially for cardiac studies.

Multi-source x-ray imaging systems offer the ability to rapidly scan an imaging volume, to modulate the dose across the imaging volume, and to generate volumetric images (albeit with anisotropic resolution) without gantry motion. Similar as for multi-source CT, these system benefits are achieved at the expense of a more complicated x-ray source subsystem. To date, distributed source prototypes utilize a stationary-anode topology due to its distributed nature. As such, maximum power capability of these systems, relative to their single-source counterparts, is limited. Reducing the dwell time per spot location and increasing the number of focal spot positions with a stationary anode help ameliorate the power deficiency; however, detector technology with fast digitization and readout speed is needed to match these more stringent source requirements. Alternatively, future distributed source concepts utilizing rotating-anode architectures are also worthy of consideration.

The applications of multi-source x-ray technology that have been considered to date have been presented above. Given the benefits and limitations, imaging applications that require low-dose x-ray exposures and multi-perspective viewing of anatomy seem well-suited for this technology. One possible x-ray imaging modality that could benefit from distributed source technology consists in fluoroscopic acquisitions during interventional imaging. With this imaging modality, minimally invasive procedures are used to diagnose and/or treat disease. Clinical workflows include interventional cardiology (for example, diagnosis and treatment of coronary artery disease such as the presence of a stenosis) – the proposed application of the scanned-beam area source presented above; interventional neuroradiology (for example, diagnosis and treatment of neurovascular anomalies such as an aneurism); interventional radiology (for example, therapy for cancer treatment); etc. The interventional procedure may be performed with a catheter and/or needles; the benefits to the patient are less procedure risk and less recovery time [95].

During an interventional procedure, a gantry, such as C-arm gantry to facilitate access to the patient, may need repositioning to better visualize the imaged anatomy, for example to better visualize navigation of a catheter through a tortuous vessel. Additionally, it may be desirable to rotate the C-arm gantry to acquire projection data for a limited angular range to perform tomosynthesis imaging. In both circumstances, a distributed source could facilitate such procedures without gantry relocation. Moreover, the tomosynthesis reconstructions of the anatomy could be updated as necessary by the interventionalist. This capability would enable the clinician to better visualize the anatomy to facilitate the given procedure. However, a remaining concern is the inability of the source architecture to provide high flux for acquisition of diagnostic images of record.

To facilitate acquisition of projection data over a larger angular coverage without gantry rotation, a distributed source comprising multiple electron emitters has a smaller footprint, when compared to a scanned-beam electron source providing comparable angular coverage since the section of the vacuum vessel required for steering the electron beam is obviated. Conversely, since a scanned electron beam source comprises thousands of x-ray focal spots over a large surface area of the anode, the average power capability of such a system is likely to be higher with reduced complexity than a distributed source utilizing multiple electron beams.

Practical multi-beam sources may require a very large number of electron beams (>100s). Improved target technologies, as well as reliable cold cathode devices, need to be made available; as such, significant research, development, and manufacturing investments are required. Although novel target technologies are actively being studied, the scientific community is yet to make a major breakthrough in the quest for identifying the low-cost, reliable, robust, high-emission and long-life cold cathode/field emitter. However researchers worldwide are still proposing promising electron emitter concepts: nano-Spindt emitters (successfully explored for displays [96]), pyroelectric emitters (already demonstrated in initial commercial products [97]), etc., while envisioning the ideal, compact, 2D flat-panel distributed x-ray source that may one day become the standard of care in x-ray imaging applications. As television sets transformed in several tens of years from the large, costly, bulky devices into very thin, compact, light and low-cost commercial offerings, one may dream of this ultimate flat-panel x-ray source to become reality sometimes in the not too distant future.

To date, collaborative efforts between x-ray source designers and major imaging equipment manufacturers have resulted in some investigative studies of such systems; however, no clinical product utilizing a distributed source has been yet released by the major imaging equipment manufacturers.

ACKNOWLEDGMENTS

The authors of this paper are grateful for the help provided by Xi Zhang – GE Global Research (for help on target cal-

culations and editing), Denise Largen – GE Global Research for editing and Carey Rogers – GE Healthcare for critical revisions and suggestions. The content is solely the responsibility of the authors and does not necessarily represent the official views of the National Institute of Biomedical Imaging and Bioengineering or the National Institutes of Health

REFERENCES

[1] W. H. Berninger and R. W. Redington, "Multiple purpose high speed tomographic X-ray scanner," U.S. Patent 4 196 352A, Apr. 1, 1980.
[2] R. A. Robb, "The dynamic spatial reconstructor: An X-ray video-fluoroscopic CT scanner for dynamic volume imaging of moving organs," *IEEE Trans. Med. Imag.*, vol. 1, no. 1, pp. 22–33, Jul. 1982.
[3] T. G. Flohr *et al.*, "First performance evaluation of a dual-source CT (DSCT) system," *Eur. Radiol.*, vol. 16, no. 2, pp. 256–268, 2006.
[4] M. Lell *et al.*, "Prospectively ECG-triggered high-pitch spiral acquisition for coronary CT angiography using dual source CT: Technique and initial experience," *Eur. Radiol.*, vol. 19, no. 11, pp. 2576–2583, 2009.
[5] T. R. Johnson *et al.*, "Material differentiation by dual energy CT: Initial experience," *Eur. Radiol.*, vol. 17, no. 6, pp. 1510–1517, 2007.
[6] Y. Kyriakou and W. A. Kalender, "Intensity distribution and impact of scatter for dual-source CT," *Phys. Med. Biol.*, vol. 52, no. 23, pp. 6969–6989, 2007.
[7] K. J. Engel, C. Herrmann, and G. Zeitler, "X-ray scattering in single- and dual-source CT," *Med. Phys.*, vol. 35, no. 1, pp. 318–332, 2008.
[8] J. W. Eberhard, "Dual parallel cone beam circular scanning trajectories for reduced data incompleteness in three-dimensional computerized tomography," U.S. Patent 5 068 882, Nov. 26, 1991.
[9] R. K. O. Behling, "Multiple focal spot X-ray tube with multiple electron beam manipulating units," U.S. Patent 7 949 102, May 24, 2011.
[10] J. S. Price, W. Block, and M. Vermilyea, "Extended multi-spot computed tomography X-ray source," U.S. Patent 6 983 035, Jan. 3, 2006.
[11] N. Pelc, "Volumetric computed tomography (VCT)," U.S. Patent 7 072 436, Jul. 4, 2006.
[12] E. Dafni, "X-ray tube," U.S. Patent 8 693 638, Apr. 8, 2014.
[13] C. Mistretta, S. Patch, R. Boutchko, and J. Hsieh, "Computed tomography with z-axis scanning," U.S. Patent 20 050 100 126, May 12, 2005.
[14] H. Morgan, "Rotating anode x-ray tube with multiple simultaneously emitting focal spots," U.S. Patent 6 125 167, Sep. 26, 2000.
[15] B. De Man and S. Basu, "Method and apparatus for employing multiple axial sources," U.S. Patent 7 639 774, Dec. 29, 2009.
[16] G. Cao, J. Zhang, O. Zhou, and J. Lu, "Temporal multiplexing radiography for dynamic X-ray imaging," *Rev. Sci. Instrum.*, vol. 80, no. 9, p. 093902, 2009.
[17] B. De Man, N. J. Pelc, C. Dumoulin, and T. Bernstein, "Propagation of quantum noise in multiplexed X-ray imaging," *Proc. SPIE*, vol. 6913, p. 69131U, Mar. 2008.
[18] Z. Yin, B. De Man, and J. Pack, "Analytical cone-beam reconstruction using a multi-source inverse geometry CT system," *Proc. SPIE*, vol. 6510, p. 651021, Mar. 2007.
[19] Z. Yin, B. De Man, and J. Pack, "3D analytic cone-beam reconstruction for multiaxial CT acquisitions," *Int. J. Biomed. Imag.*, vol. 2009, Jan. 2009, Art. ID 538389.
[20] R. Boutchko, C. Mistretta, G.-H. Chen, J. Hsieh, and S. K. Patch, "Z-scan: Feasibility study of an ultrafast volume CT scanner," in *Proc. Fully 3D Meeting*, p. TUPM 2–8, 2003.
[21] H. Xu, "A study on concave-X-ray-source-based direct volumetric imaging from single scan," Ph.D. thesis, 2002.
[22] T. G. Schmidt, R. Fahrig, N. J. Pelc, and E. G. Solomon, "An inverse-geometry volumetric CT system with a large-area scanned source: A feasibility study," *Med. Phys.*, vol. 31, no. 9, pp. 2623–2627, 2004.
[23] B. De Man *et al.*, "Multi-source inverse geometry CT: A new system concept for X-ray computed tomography," *Proc. SPIE*, vol. 6510, p. 65100H, Mar. 2007.
[24] B. De Man, P. M. Edic, and S. Basu, "Method and system for imaging using multiple offset X-ray emission points," U.S. Patent U.S. 7 333 587, Feb. 19, 2008.
[25] B. De Man *et al.*, "Multi-source inverse-geometry CT: From system concept to research prototype," in *Proc. IEEE Nucl. Sci. Symp. Med. Imag. Conf.*, Orlando, FL, USA, Oct./Nov. 2009, pp. 3531–3533.
[26] J. Uribe *et al.*, "Multi-source inverse-geometry CT: Prototype system integration," in *Proc. IEEE Nucl. Sci. Symp. Med. Imag. Conf.*, Knoxville, TN, USA, Oct./Nov. 2010, pp. 2578–2581.
[27] J. Baek *et al.*, "Initial results with a multisource inverse-geometry CT system," *Proc. SPIE*, vol. 8313, p. 83131A, Feb. 2011.
[28] J. Sperl, D. Bequé, B. Claus, B. De Man, B. Senzig, and M. Brokate, "Computer-assisted scan protocol and reconstruction (CASPAR)—Reduction of image noise and patient dose," *IEEE Trans. Med. Imag.*, vol. 29, no. 3, pp. 724–732, Mar. 2010.
[29] D. Boyd *et al.*, "High-speed, multi-slice, X-ray computed tomography," *Proc. SPIE*, vol. 372, pp. 139–150, Nov. 1982.
[30] B. De Man *et al.*, "Stationary computed tomography system and method," U.S. Patent 7 280 631, Oct. 9, 2007.
[31] Y. Bresler and N. P. Willis, "Optical scan design for time-varying tomographic imaging," 1993.
[32] Q. Zhao, "Methods and apparatus for image reconstruction in distributed X-ray source CT systems," U.S. Patent 6 937 689, Aug. 30, 2005.
[33] E. Morton, "Ultrafast 3D reconstruction for X-ray real-time tomography (RTT)," in *Proc. IEEE Med. Imag. Conf.*, Oct./Nov. 2009, pp. 4077–4080.
[34] J. Wang, P. Fitzgerald, H. Gao, Y. Jin, G. Wang, and B. De Man, "Stationary and non-stationary multi-beamline architecture study for cardiac CT imaging," in *Proc. SPIE, Med. Imag., Phys. Med. Imag.*, vol. 9033. Apr. 2014.
[35] S. S. Hsieh *et al.*, "The feasibility of an inverse geometry CT system with stationary source arrays," *Med. Phys.*, vol. 40, no. 3, p. 031904, 2013.
[36] Z. Yin and B. De Man, "X-ray computed tomography with asynchronous source and detector rotation," presented at World Congr. Med. Phys., Seoul, Korea, 2006.
[37] G. M. Besson, "Old ideas new again: A system concept for fast CT using semi-conventional approaches," in *Proc. Fully 3D Meeting*, 2014, p. 303.
[38] F. Sprenger *et al.*, "Distributed source X-ray tube technology for tomosynthesis imaging," *Proc. SPIE*, vol. 7622, p. 76225M, Mar. 2010.
[39] M. A. Speidel, "Inverse geometry X-ray imaging: Application in interventional procedures," *J. Amer. College Radiol.*, vol. 8, no. 1, pp. 74–77, Jan. 2011.
[40] X. Qian *et al.*, "High resolution stationary digital breast tomosynthesis using distributed carbon nanotube X-ray source array," *Med. Phys.*, vol. 39, no. 4, pp. 2090–2099, Apr. 2012.
[41] J. Shan *et al.*, "Stationary chest tomosynthesis using a CNT X-ray source array," *Proc. SPIE*, vol. 8668, p. 86680E, Mar. 2013.
[42] J. Shan *et al.*, "Evaluation of imaging geometry for stationary chest tomosynthesis," *Proc. SPIE*, vol. 9033, p. 903317, Mar. 2014.
[43] The National Lung Screening Trial Research Team, "Reduced lung-cancer mortality with low-dose computed tomographic screening," *New England J. Med.*, vol. 365, no. 5, pp. 395–409, Aug. 2011.
[44] (Dec. 2013). *Screening for Lung Cancer, U.S. Preventive Services Task Force Recommendation Statement*. [Online]. Available: http://www.uspreventiveservicestaskforce.org/uspstf13/lungcan/lungcanfinalrs.htm
[45] D. Habermehl, K. Henkner, S. Ecker, O. Jäkel, J. Debus, and S. E. Combs, "Evaluation of different fiducial markers for image-guided radiotherapy and particle therapy," *J. Radiat. Res.*, vol. 54, pp. i61–i68, Jul. 2013.
[46] P. Schardt *et al.*, "New X-ray tube performance in computed tomography by introducing the rotating envelope tube technology," *Med. Phys.*, vol. 31, no. 9, pp. 2699–2706, 2004.
[47] J. M. Bonard, C. Klinke, K. A. Dean, and B. F. Coll, "Degradation and failure of carbon nanotube field emitters," *Phys. Rev. B*, vol. 67, no. 11, p. 115406, Mar. 2003.
[48] J. A. Nation *et al.*, "Advances in cold cathode physics and technology," *Proc. IEEE*, vol. 87, no. 5, pp. 865–889, May 1999.
[49] D. Temple *et al.*, "Fabrication of column-based silicon field emitter arrays for enhanced performance and yield," *J. Vac. Sci. Technol. B, Microelectron. Nanometer Struct.*, vol. 13, no. 1, pp. 150-157, Jan. 1995.
[50] S. H. Jo, J. Y. Lao, Z. F. Ren, R. A. Farrer, T. Baldacchini, and J. T. Fourkas, "Field-emission studies on thin films of zinc oxide nanowires," *Appl. Phys. Lett.*, vol. 83, no. 23, p. 4821, 2003.
[51] X. T. Zhou *et al.*, "Growth and emission properties of beta-SiC nanorods," *Mater. Sci. Eng. A, Struct. Mater., Properties, Microstruct. Process.*, vol. 286, no. 1, pp. 119–124, Jun. 2000.
[52] F. G. Tarntair *et al.*, "Field emission from quasi-aligned SiCN nanorods," *Appl. Phys. Lett.*, vol. 76, no. 18, p. 2630, 2000.
[53] S. W. Lee, S. S. Lee, and E.-H. Yang, "A Study on field emission characteristics of planar graphene layers obtained from a highly oriented pyrolyzed graphite block," *Nanosc. Res. Lett.*, vol. 4, pp. 1218–1221, Jul. 2009.
[54] D. Ye, S. Moussa, J. D. Ferguson, A. A. Baski, and M. S. El-Shall, "Highly efficient electron field emission from graphene oxide sheets supported by nickel nanotip arrays," *Nano Lett.*, vol. 12, no. 3, pp. 1265–1268, 2012.

[55] P. R. Schwoebel, J. M. Boone, and J. Shao, "Studies of a prototype linear stationary X-ray source for tomosynthesis imaging," *Phys. Med. Biol.*, vol. 59, no. 10, pp. 2393–2413, 2014.
[56] S. Wang, X. Calderon, R. Peng, E. C. Schreiber, O. Zhou, and S. Chang, "A carbon nanotube field emission multipixel X-ray array source for micro-radiotherapy application," *Appl. Phys. Lett.*, vol. 98, no. 21, p. 213701, May 2011.
[57] G. Yang *et al.*, "Stationary digital breast tomosynthesis system with a multi-beam field emission X-ray source array," *Proc. SPIE*, vol. 6913, p. 69131A, Mar. 2008.
[58] F. Sprenger *et al.*, "Stationary digital breast tomosynthesis with distributed field emission X-ray tube," *Proc. SPIE*, vol. 7961, p. 878280, Mar. 2011.
[59] X. Qian *et al.*, "Design and characterization of a spatially distributed multibeam field emission X-ray source for stationary digital breast tomosynthesis," *Med. Phys.*, vol. 36, no. 10, pp. 4389–4399, 2009.
[60] X. Xu, J. Kim, P. Laganis, D. Schulze, Y. Liang, and T. Zhang, "A tetrahedron beam computed tomography benchtop system with a multiple pixel field emission X-ray tube," *Med. Phys.*, vol. 38, no. 10, pp. 5500–5508, 2011.
[61] O. Zou, "Presentation at the X-ray source workshop," presented at the X-ray Sour. Workshop SPIE Med. Imag. Conf., 2014.
[62] A. W. Tucker, Y. Z. Lee, C. M. Kuzmiak, J. Calliste, J. Lu, and O. Zhou, "Increased microcalcification visibility in lumpectomy specimens using a stationary digital breast tomosynthesis system," *Proc. SPIE*, vol. 9033, p. 903316, Mar. 2014.
[63] K. Frutschy *et al.*, "X-ray multisource for medical imaging," *Proc. SPIE*, vol. 7258, Mar. 2009, Art. ID 725822.
[64] K. Frutschy *et al.*, "High power distributed X-ray source," *Proc. SPIE*, vol. 7622, p. 76221H, Mar. 2010.
[65] J. Uribe *et al.*, "Multisource inverse-geometry CT—Prototype system integration," in *Proc. IEEE Nucl. Sci. Symp. Conf. Rec. (NSS/MIC)*, Knoxville, TN, USA, Oct./Nov. 2010, pp. 2578–2581.
[66] J. Baek *et al.*, "Initial results with a multisource inverse-geometry CT system," *Proc. SPIE, Med. Imag., Phys. Med. Imag.*, vol. 8313, p. 83131A, Feb. 2012.
[67] J. Baek *et al.*, "A multi-source inverse-geometry CT system: Initial results with an 8 spot X-ray source array," *Phys. Med. Biol.*, vol. 59, no. 5, pp. 1189–1202, 2014.
[68] V. B. Neculaes *et al.*, "Design and characterization of electron beam focusing for X-ray generation in novel medical imaging architecture," *Phys. Plasmas*, vol. 21, no. 5, p. 056702, 2014.
[69] A. Caiafa, J. A. Sabate, and E. Delgado, "Low-ripple low-transition time, current driver for large inductive loads," in *Proc. 32nd Annu. Conf. IEEE Ind. Electron. (IECON)*, Nov. 2006, pp. 2077–2083.
[70] J. Zhang *et al.*, "Stationary scanning X-ray source based on carbon nanotube field emitters," *Appl. Phys. Lett.*, vol. 86, no. 18, p. 184104, 2005.
[71] Y. Zou, M. E. Vermilyea, L. P. Inzinna, and A. Caiafa, "Virtual matrix control scheme for multiple spot X-ray source," U.S. Patent 7 826 594, Nov. 2, 2010.
[72] W. D. Coolidge, "X-ray apparatus," U.S. Patent 1 215 116 A, Feb. 6, 1917.
[73] W. J. Oosterkamp, "The heat dissipation in the anode of an X-ray tube," *Philips Res.*, vol. 3, pp. 49–59, 1985.
[74] J. Shan, O. Zhou, and J. Lu, "Anode thermal analysis of high power microfocus CNT X-ray tubes for *in vivo* small animal imaging," *Proc. SPIE, Med. Imag., Phys. Med. Imag.*, vol. 8313, pp. 83130O-1–83130O-9, Mar. 2012.
[75] V. Bogdan Neculaes *et al.*, "Multi-source inverse-geometry CT—Part 2: X-ray source design and prototype," *Med. Phys.*
[76] A. Ganguly and N. J. Pelc, "On the angular dependence of bremsstrahlung X-ray emission," *Proc. SPIE, Med. Imag., Phys. Med. Imag.*, vol. 6913, p. 69134P, Mar. 2008.
[77] D. Hill, "Electron beam CT of the heart," in *CT of the Heart: Principles and Applications* (Contemporary Cardiology). New York, NY, USA: Springer-Verlag, 2005.
[78] E. Gidcumb, B. Gao, J. Shan, C. Inscoe, J. Lu, and O. Zhou, "Carbon nanotube electron field emitters for X-ray imaging of human breast cancer," *Nanotechnology*, vol. 25, no. 24, p. 245704, 2014.
[79] M. A. Speidel, B. P. Wilfley, J. M. Star-Lack, J. A. Heanue, and M. S. Van Lysel, "Scanning-beam digital X-ray (SBDX) technology for interventional and diagnostic cardiac angiography," *Med. Phys.*, vol. 33, no. 8, pp. 2714–2727, 2006.
[80] M. A. Speidel, B. P. Wilfley, J. M. Star-Lack, J. A. Heanue, T. D. Betts, and M. S. Van Lysel, "Comparison of entrance exposure and signal-to-noise ratio between an SBDX prototype and a wide-beam cardiac angiographic system," *Med. Phys.*, vol. 33, no. 8, pp. 2728–2743, 2006.
[81] Radius Health, Stellarray, CSEM, and GE Measurement & Control Solutions. [Online]. Available: http://www.radius-health.com/
[82] Radius Health, Stellarray, CSEM, and GE Measurement & Control Solutions. [Online]. Available: http://stellar-ray.com/
[83] Radius Health, Stellarray, CSEM, and GE Measurement & Control Solutions. [Online]. Available: http://www.csem.ch/docs/show.aspx/16028/docname/NextGenXRaySystems.pdf
[84] Radius Health, Stellarray, CSEM, and GE Measurement & Control Solutions. [Online]. Available: http://www.ge-mcs.com/download/x-ray/phoenix-x-ray/diamond_window%20GEIT-31340EN%200910_low.pdf
[85] T. Tuohimaa, M. Otendal, and H. M. Hertz, "Phase-contrast X-ray imaging with a liquid-metal-jet-anode microfocus source," *Appl. Phys. Lett.*, vol. 91, no. 7, p. 074104, 2007.
[86] M. Sridhar, M. Venugopal, D. Mishra, S. Sebastian, H. Vadari, and M. Frontera, "High flux X-ray target and assembly," U.S. Patent 7 751 530, Jul. 6, 2010.
[87] T. Raber, B. Bernard, T. Andrew, W. Bin, W. Colin R., B. Mark, and B. Ernest, "X-ray anode focal track region," U.S. Patent 7 356 122, Apr. 8, 2008.
[88] J. E. Simpson, M. Vermilyea, and C. Wilson, "Rotating notched transmission X-ray for multiple focal spots," U.S. Patent 6 947 522, Sep. 20, 2005.
[89] L. R. Falce and R. L. Ives, "Sintered wire annode," U.S. Patent 7 313 226, Dec. 25, 2007.
[90] J. Uribe *et al.*, "Multisource inverse-geometry CT—Prototype system integration," in *Proc. IEEE Nucl. Sci. Symp. Conf. Rec. (NSS/MIC)*, Oct./Nov. 2010, pp. 2578–2581.
[91] G. Wang and H. Yu, "The meaning of interior tomography," *Phys. Med. Biol.*, vol. 58, no. 16, p. R161, 2013.
[92] G. Wang, H. Yu, and Y. Ye, "A scheme for multisource interior tomography," *Med. Phys.*, vol. 36, no. 8, p. 3575, Aug. 2009.
[93] G. Wang, Y. Liu, Y. Ye, S. Zhao, J. Hsieh, and S. Ge, "Top-level design and preliminary physical analysis for the first electron-beam micro-CT scanner," *J. X-Ray Sci. Technol.*, vol. 12, no. 4, pp. 251–260, 2004.
[94] C. Wu, Y. Cheng, Y. Ding, F. Wei, and Y. Jin, "A novel X-ray computed tomography method for fast measurement of multiphase flow," *Chem. Eng. Sci.*, vol. 62, no. 16, pp. 4325–4335, Aug. 2007.
[95] Johns Hopkins Medicine. [Online]. Available: http://www.hopkinsmedicine.org/vascular/what_is_IR.html
[96] M. Rose and Y. Fan, "New field emission technologies," in *Handbook of Visual Display Technology*. Berlin, Germany: Springer-Verlag, 2012, pp. 1105–1136.
[97] Amp Tek. [Online]. Available: http://www.amptek.com/products/cool-x-pyroelectric-x-ray-generator/

VASILE BOGDAN NECULAES received B.S. and M.S. degrees in Physics from "Al. I Cuza University" (Iasi, Romania), and M.S. and PhD degrees in Nuclear Engineering and Radiological Sciences from University of Michigan. Currently, Dr. Neculaes is a senior physicist in the High Energy Physics Laboratory at GE Global Research in Niskayuna, NY. Dr. Neculaes' expertise covers physics based applications in medical imaging, biology, biomedical instrumentation and beyond. He led one of the largest X-ray source programs at GEGR in the recent decades that delivered, with funding from GEGR and NIH, the first in the world distributed X-ray source for inverse geometry computed tomography. He has also led the first successful X-ray source demonstrations with carbon nanotube cold cathodes at GEGR. He has initiated and chaired the bioelectromagnetics initiative at GEGR, a multidisciplinary research platform focused on creating novel electromagnetic means for manipulation of biological samples. His teams demonstrated new means for cell permeabilization using infrared lasers to enable exogenous molecule delivery, novel gene delivery methods *in vitro* using magnetic nanoparticles and magnetic fields, and innovative ex-vivo platelet activation techniques with pulse electric fields for autologous wound healing applications in clinical workflows. He has authored numerous peer-reviewed articles in prestigious peer-reviewed journals, while being awarded seven patents. His latest peer-reviewed papers unveil new thermal gradient mechanisms at the cell membrane upon interaction with pulse electric fields, and growth factor release from platelets when activated via electrical pulse stimulation.

PETER M. EDIC received the A.A.S. degree in electrical engineering technology from Mohawk Valley Community College, Utica, NY, USA, in 1987, the B.S. degree in electrical engineering from Syracuse University, Syracuse, NY, USA, in 1990, and the M.S. and Ph.D. degrees in electrical engineering from the Rensselaer Polytechnic Institute (RPI), Troy, NY, USA, in 1991 and 1994, respectively. His Ph.D. research topic was the implementation of a real-time electrical impedance tomography. After completing post-doctoral research at RPI and the Department of Biomedical Engineering, Becton Dickinson, RPI, he joined GE Global Research, Niskayuna, NY, USA, in 1995, where he is currently a Principal Engineer with CT, X-ray, and Functional Imaging Technology Organization. His research interests include advanced research topics in computed tomography (CT), including advanced cardiac imaging, dual-energy imaging, photon counting CT, and interventional imaging.

MARK FRONTERA received the M.E. degree in mechanical engineering, and is currently the Manager of the High Energy Physics Laboratory with CT, X-ray, and Functional Imaging Organization, GE Global Research, Niskayuna, NY, USA. His expertise includes X-ray sources for healthcare and inspection applications. He has over 10 years of experience in this domain leading programs delivering new commercial technology in X-ray targets, cathodes, X-ray source subsystems, power electronics, and high-voltage generators. He holds 16 U.S. patents. He is a Six Sigma Black Belt and has received certification as a Level 3 TRIZ Practitioner.

ANTONIO CAIAFA received the Ph.D. degree from the University of South Carolina-Columbia, Columbia, SC, USA, in 2004. He joined GRC in 2004. He is currently the leading expert in high-voltage electronics with GE Global Research (GEGR), Niskayuna, NY, USA. As a Senior Research Scientist, his research has impacted several application areas and has led to various GEGR products, both in medical imaging and luggage scanning. He has numerous conference publications and journal articles, and he holds 28 U.S. patent applications.

GE WANG (F'03) received the Ph.D. degree in electrical, computer, and systems engineering, and is currently the Clark and Crossan Endowed Chair Professor and the Director of the Biomedical Imaging Center/Cluster, Rensselaer Polytechnic Institute, Troy, NY, USA. His expertise includes X-ray computed tomography (CT) and optical molecular tomography. He wrote the pioneering papers on the first spiral cone-beam CT algorithm (1991 and 1993) that enables spiral/helical cone-beam CT imaging, which is constantly used in almost all hospitals worldwide. There are over 70 million CT scans yearly in the U.S. alone, with a majority in the spiral cone-beam/multislice mode. He and his collaborators also wrote the first paper on bioluminescence tomography, creating a new area of optical molecular tomography. His group published the first papers on interior tomography and omnitomography for grand fusion of all relevant tomographic modalities (*all-in-one*) to acquire different datasets simultaneously (*all-at-once*) and capture multiphysics interactions (*all-of-couplings*) with simultaneous CT-MRI and simultaneous CT-SPECT as special examples. His results were featured in *Nature*, *Science*, and *Proceedings of the National Academy of Sciences*, and recognized with various academic awards. He has authored about 400 journal papers. His group has been in close collaboration with multiple world-class groups, and continuously funded by federal agents ($25 MasPI/ContactPI/Multi-PI, 28M$ as Co-PI/Co-I/Mentor). He is the lead Guest Editor of four IEEE TRANSACTIONS ON MEDICAL IMAGING Special Issues on X-ray CT, molecular imaging, compressive sensing, and spectral CT, respectively, the Founding Editor-in-Chief of the *International Journal of Biomedical Imaging*, and an Associate Editor of the IEEE TRANSACTIONS ON MEDICAL IMAGING and *Medical Physics Journal*. He is a fellow of the International Society for Optics and Photonics, the Optical Society of America, the American Institute for Medical and Biological Engineering, and the American Association of Physicists in Medicine.

BRUNO DE MAN received the B.S., M.S., and Ph.D. degrees in electrical engineering from Katholieke Universiteit Leuven, Leuven, Belgium, in 1995, 1995, and 2001, respectively. During his Ph.D. work, he pioneered the use of statistical iterative reconstruction methods for computed tomography (CT), developed accurate CT simulation models, and studied new methods for metal artifact reduction. After he joined GE Global Research (GEGR), Niskayuna, NY, USA, in 2001, he continued his research in CT iterative reconstruction in collaboration with the University of Michigan, Ann Arbor, MI, USA, Purdue University, West Lafayette, IN, USA, and the University of Notre Dame, Notre Dame, IN, USA. This work led to the commercial introduction of Veo by GE Healthcare (GEHC) in 2010. He is known for the development of distance-driven projection, a technique that was adopted in both the CT and PET industry. He was one of the two original authors of CatSim, a CT simulation package widely used by GEGR and academic partners. He was a part of the team that developed the reconstruction algorithms used on the recent GEHC CT product scanners. In collaboration with Stanford University, Stanford, CA, USA, he and his team developed the first multisource inverse-geometry CT scanner. He also has a long-term collaboration with the Rensselaer Polytechnic Institute, Troy, NY, USA (formerly with the Virginia Polytechnic Institute and State University, Blacksburg, VA, USA, and Wake Forest University, Winston-Salem, NC, USA) to develop novel cardiac CT architectures, with the University of Washington, Seattle, WA, USA, to develop ultralow-dose techniques for PET-CT attenuation correction and the Massachusetts General Hospital, Boston, MA, USA, to develop organ targeting and adaptive sequencing for sub-mSv imaging. He is currently the Manager of the CT Systems and Applications Laboratory and CT Research Portfolio Leader with GEGR. He holds 99 U.S. patent applications and has authored over 100 international publications.